Agricultural Water Management 266 (2022) 107572

Contents lists available at ScienceDirect

Agricultural Water Management

journal homepage: www.elsevier.com/locate/agwat

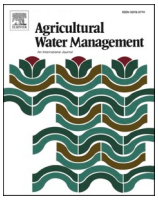

Water uptake dynamics in apple trees assessed by an isotope labeling approach

A. Aguzzoni [a,b,*], M. Engel [a,1], D. Zanotelli [a], D. Penna [c], F. Comiti [a], M. Tagliavini [a]

[a] Faculty of Science and Technology, Free University of Bozen-Bolzano, Bolzano, Italy
[b] Eco-Research, Bolzano, Italy
[c] Department of Agriculture, Food, Environment and Forestry (DAGRI), University of Florence, Florence, Italy

ARTICLE INFO

Handling Editor - Dr. B.E. Clothier

Keywords:
Irrigation water
Soil water
Root water uptake
Isotope analysis
Deuterium tracing

ABSTRACT

Improving our knowledge on the relative contribution of irrigation water, precipitation, and groundwater to tree transpiration is necessary for an efficient and sustainable use of water resources in agriculture. For this purpose, we applied deuterium (^{2}H) enriched water to trace the uptake of irrigation water by apple trees under field and pot conditions. ^{2}H-enriched water was supplied to apple trees in an Alpine valley mimicking sprinkler irrigation. Labeled water infiltration in the soil and presence in apple tree shoots was measured over a week. An ancillary experiment using potted trees was performed to elucidate the role of irrigation water after soil saturation with ^{2}H-enriched water. Under field conditions, ^{2}H-enriched water infiltrated to a maximum depth of 0.6 m, where most of the fine roots were present, and mixed with pre-irrigation soil water. Sprinkler irrigation water was taken up by apple trees 2–4 h after its supply and its contribution to the shoot water content increased in the first 24 h, then it leveled off. Tree water absorbed from the enriched soil layer represented on average 48 ± 3% and 26 ± 2% of the total water in shoot axes and leaves, respectively. The results of the pot experiment confirmed the contribution of irrigation water to shoot water and allowed us to speculate that under field conditions groundwater (ca. 0.9 m deep, with capillary rise expected up to 0.6 m depth) did not significantly contribute to tree water uptake. Results indicate that a large fraction of shoot water (52–74%) did not derive from recent soil water uptake, suggesting a rather limited water mixing within tree organs.

1. Introduction

Improving water management strategies in agriculture is pivotal to face future scenarios characterized by an increased extension of irrigated crops and a concurrent decrease in freshwater availability (Chartzoulakis and Bertaki, 2015). In this context, a better understanding of the dynamics of water uptake by crops and water use from multiple water pools (e.g., precipitation, irrigation, groundwater) to satisfy crop water requirements is highly necessary. Despite the extensive literature on crop irrigation, the actual contribution of irrigation water to plant transpiration is still uncertain. Similarly, the quantitative contribution of the different water sources to the overall water uptake by trees is unclear. Studies investigating these aspects have to face the complexity of soil water processes, subjected to temporal and spatial variability (Jackisch et al., 2020; Li et al., 2014).

Hydrogen and oxygen isotopes in the water molecule represent a reliable tracer of water source and its movements, providing information about water fluxes in the soil-plant-atmosphere continuum (SPAC) (Penna et al., 2020; Sprenger et al., 2016). In the last decades, many authors studied the water uptake dynamics comparing the isotopic composition of plant water and that of the main local water sources, mostly through the application of mixing models (Rothfuss and Javaux, 2017). Several isotope-based studies analyzed root water uptake and the proportional contribution of different water sources and/or irrigation practices, in relation to plant species, growth stage, and the depth of their root system (Cao et al., 2018; Liu et al., 2020; Mahindawansha et al., 2018; Wu et al., 2018). However, the outcomes of these studies are affected by several factors, including the sampling representativeness of all the available water sources, the necessity for a sufficiently appreciable difference in the isotopic composition of each water source, in addition to methodological constraints (Berry et al., 2018; Beyer and Penna, 2021; Orlowski et al., 2016a). Moreover, this approach is valid

* Corresponding author at: Eco-Research, Bolzano, Italy.
E-mail address: a.aguzzoni@eco-research.it (A. Aguzzoni).
[1] Present address: Federal Institute of Hydrology, Radiology and Water Monitoring, Koblenz, Germany.

https://doi.org/10.1016/j.agwat.2022.107572
Received 17 December 2021; Received in revised form 18 February 2022; Accepted 23 February 2022
Available online 5 March 2022

assuming that no isotope fractionation occurs during root uptake (Ehleringer and Dawson, 1992). This assumption was questioned by several authors, who measured an appreciable isotope fractionation in several tree species in relation to water movements at the soil-root interface and within plants (Ellsworth and Williams, 2007; Poca et al., 2019; Zhao et al., 2016). Recently, water isotope heterogeneity both in the soil pores and tree stems was found to contribute to soil-stem isotope offsets, which might cause an incorrect interpretation of isotope data (Barbeta et al., 2019, 2020, 2022). It is therefore evident that the above-mentioned factors may hinder the identification of tree water sources when different water pools exist, especially under natural environmental conditions (Beyer and Penna, 2021).

The use of deuterium (^{2}H) enriched water makes possible to artificially modify the isotopic composition of a water reservoir and trace its uptake by plants, without altering the water chemical and physical properties (Becker and Coplen, 2001). Being part of the water molecule, ^{2}H is a conservative tracer and due to its low natural abundance (ca. 0.015%), small additions of heavy water (^2H_2O) in a confined environment can be successfully monitored after equilibration with local water (Becker and Coplen, 2001). Adding an excess of ^{2}H overcomes also the problem of potential isotope fractionation from the water source to the tree organs, as the fractionation would result rather negligible compared to the measurable artificial enrichment (Beyer et al., 2016; Rowland et al., 2008).

In the past years, the application of ^{2}H-enriched water in isotope-based studies has encompassed several aspects related to ecohydrological studies, including, among the others, soil water accessed by plants (e.g. Bogie et al., 2018; Beyer et al., 2018; Rasmussen et al., 2020), temporal dynamics of tree water (Seeger and Weiler, 2021), water transport and distribution in trees under specific irrigation regimes (Liu et al., 2014; Rowland et al., 2008), and soil water movements (e.g. Mali et al., 2007; Koeniger et al., 2010; Grünberger et al., 2011). Nonetheless, most of these studies were conducted in forest ecosystems, with only a few applications regarding agricultural systems. To the best of our knowledge, none of the previous studies provided an in-depth analysis of the role of irrigation water compared to other water pools in relation to plant water needs and, hence, the quantification and comprehension of irrigation water uptake dynamics remain weak.

The present study is a follow-up of a previous research aimed at identifying the prevailing water sources for apple trees in an Alpine valley of South Tyrol in Northern Italy applying a stable isotope approach (Penna et al., 2021). In this area, intensive apple cultivation is widespread and, to guarantee high fruit yield and quality, irrigation water is frequently applied for most of the growing season. To optimize irrigation water use, it is necessary to evaluate its contribution to tree water in comparison with other locally available water sources, such as rainwater and groundwater. The latter – if shallow enough – might positively contribute to soil water recharge in the root zone through capillary rising processes (Grashey-Jansen, 2010). To better understand the role of irrigation water in apple orchards and its contribution to tree water requirements in the summer period, we designed two experiments using ^{2}H-enriched irrigation water. The two labeling experiments addressed the following research questions:

1. What is the fate of the irrigation water in the soil?
2. To what extent do irrigation water and groundwater contribute to the overall tree water?

2. Materials and methods

2.1. Experiment 1 – field-grown apple trees

2.1.1. Site description

Experiment 1 was carried out in July 2019 in an apple orchard (*Malus domestica*, cv. Pinova on M9 rootstock) located in the Municipality of Laas/Lasa (German and Italian name, respectively) in the Vinschgau/Venosta Valley (South Tyrol, Italy) and close to the Adige River channel (elevation 868 m a.s.l.; size 5000 m^2). The apple orchard was planted in 2005 and was in full production in 2019 (ca. 70 ton ha^{-1}), with a north-south row orientation, perpendicular to the direction of the river flow. The tree spacing within single rows is 0.8 m, while consecutive rows are 3 m apart. In summer, an overhead sprinkler system normally provides 20 mm of water once or twice a week, depending on the rainfall events, which are normally rather infrequent in summer in this area (the long-term precipitation record is 480 mm year^{-1}). According to the USDA classification, the soil has a silt loam texture (until 0.8 m depth), with 26.7% sand and 10.8% clay, on average (Table 1). A recent investigation on apple root distribution in the same field revealed that around 50% and around 90% of the fine roots are present in the 0–0.2 m and 0–0.6 m soil layers, respectively (Penna et al., 2021).

Meteorological data including air temperature, relative humidity, precipitations, wind speed, and net radiation were recorded by a weather station located at one edge of the orchard and are summarized in Supplementary Table S1. Starting from meteorological data, the reference crop evapotranspiration (ET_0) was calculated at hourly time steps applying the FAO modified version of the Penman-Monteith equation (Allen et al., 1998, 2006).

2.1.2. Experimental design

Four consecutive tree rows were selected and, in the middle of each row, a block of three trees was chosen (hereafter called experimental unit). The selected trees were similar in tree height (ca. 3.5 m) and crown volume (ca. 3.0–3.5 m^3). The four experimental units had approximately the same distance from the river (ca. 80 m) and we assumed that the depth to groundwater table was the same for all the trees. Each experimental unit included a control tree (not-irrigated tree) and a tree to be irrigated with ^{2}H-enriched water, separated by a buffer tree (Fig. 1). A 1.3 m-long piezometer (not equipped with a level logger) was installed outside one of the experimental units to daily measure the depth of the groundwater table using a meter stick.

To create a moderate level of soil water deficit before the addition of ^{2}H-enriched water, infiltration of irrigation and rainwater was prevented covering the soil of the four experimental units with an impermeable plastic sheet (length ca. 3 m, width per row side ca. 0.8 m) from July 11 until July 23. The last irrigation cycle before covering the soil occurred on July 5 and the last rainfall on July 6 (3 mm).

On July 23 at 9 AM CET, ^{2}H-enriched water was poured into the soil of the irrigated plots. Before starting the irrigation, the plastic sheets were removed and the plots to be irrigated (1 m^2) were delimitated by plastic supports (0.1 m high) partially driven into the soil to prevent water from spreading outside of the 1 m^2 plot. ^{2}H-enriched water was prepared in 20 L cans diluting 5 mL of ^2H_2O (99.9%) into 20 L of local water ($\delta^2H = -98.8‰$) taken from an irrigation pipe close to the orchard, to reach a final δ^2H value of 1544 ± 29‰. Each tree received 40 L of water on a surface of 1 m^2 (40 mm in 15 min). Irrigation water was evenly distributed, using rain-shower watering cans, at a slow application rate to minimize runoff. No irrigation was provided to the control trees for the whole experimental period. After adding the labeled water, the plastic sheets were placed back on top of the soil and kept until the end of the experiment (July 30) to prevent irrigation water and rainwater from entering the soil of the experimental plots. A rain collector was placed at one edge of the apple orchard, outside of the tree rows, to collect rainwater from precipitations fallen during the experimental

Table 1
Experiment 1. Soil texture at different depths.

Soil layer depth (m)	Sand (%)	Silt (%)	Clay (%)
0–0.2	33	54	13
0.2–0.4	24	66	10
0.4–0.6	34	57	9
0.6–0.8	16	73	11

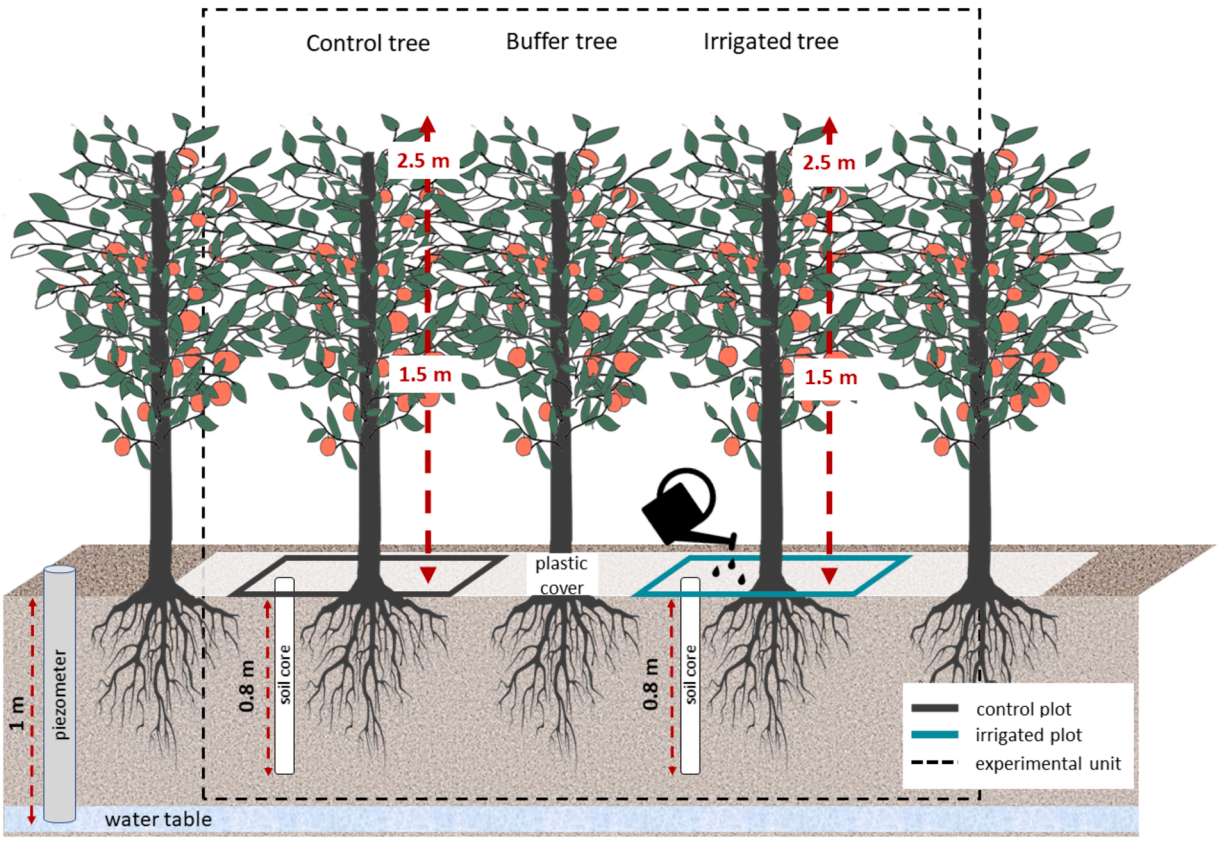

Fig. 1. Experiment 1. Schematic representation of the experimental area within a single row.

period.

2.1.3. Field sampling

Experiment 1 lasted one week after the application of the ^{2}H-enriched water. During this period, water, tree, and soil samples were collected periodically (Supplementary Table S2). Soil samples were collected 2 h after the irrigation and then at 24 h, 48 h, and 7 days (168 h) in the four irrigated and control plots using a single gauge auger (length 1 m, diameter 2.5 cm) positioned each time at 0.4 m from the tree trunk, towards one of the corners of the squared experimental plot, to a depth of 0.8 m. The soil core was then divided into 8 layers, each 0.1 m long, and a soil aliquot was sampled from each layer.

Shoot samples were collected at 2, 4, 8, 24, 48, 72, and 168 h after irrigation from the irrigated plots, both from the east and the west side of the canopy (one shoot per side, length of 10–15 cm with ca. 8 leaves), at 1.5 m and 2.5 m from the ground. Shoots sampled at 1.5 m height (hereafter referred to as "bottom" samples) were kept separate from those collected at 2.5 m (hereafter "top" samples). Two fully expanded apical leaves with petioles were immediately removed from the shoot axes and both leaves and shoot axes were then transferred into separated vials. Based on average values for the leaf area index of apple trees cultivated in this area (ca. 2.5) and the actual tree density, we estimated that the destructive shoot sampling reduced the leaf area by $< 5\%$. Hence, we assumed that such a difference did not significantly affect tree transpiration. Control trees were sampled following the same procedure used for irrigated trees at the beginning and the end of the experiment (2 and 168 h). Starting from 24 h after irrigation, tree sampling was always performed around 1–2 PM.

Both before and after the experimental period, a groundwater sample was collected from the piezometer. At the end of the experiment, rainwater collected between July 26 and 28 was sampled from the rain collector. All the collected samples were directly transferred into airtight glass vials, with a screw cap and rubber septum, sealed and stored at 4 °C until processing.

The water content of leaves and shoot axes, sampled at the end of the experiment (168 h) from both irrigated and control trees, was determined gravimetrically through the loss-on drying method (65 °C, 48 h) and expressed on a wet weight basis. The same procedure was applied to determine the moisture content of soil samples (105 °C, until constant weight), expressed on a dry weight basis (gravimetric water content) (Liu et al., 2020; Orlowski et al., 2016a).

2.1.4. Estimation of the water flux from the groundwater table

Using the soil moisture values measured in the irrigated plots at different depths and adapting Eq. (1) to a silt loam soil as indicated by Villalobos et al. (2016), the matric soil water potential at each soil depth was estimated as follows:

$$\Psi_m = \Psi_e \left(\frac{\theta_v}{\theta_{SAT}} \right)^{-b} \quad (1)$$

Where Ψ_e is the air entry water potential, which is -2.1 J kg^{-1} for silty loam soils (Villalobos et al., 2016), b an empirical parameter, which was set equal to 4.7 (Villalobos et al., 2016), θ_v (%) and θ_{SAT} (%) the volumetric and saturation water content, respectively.

Vertical water fluxes (J_w, kg m^{-2} s^{-1} and converted to mm day^{-1}) from the groundwater table to the unsaturated soil layers (from 0.8 m depth to the topsoil layer) were estimated based on the following equation (Villalobos et al., 2016):

$$J_w = -\mathrm{K}(\Psi_m) \left(\frac{d\Psi_m}{dz} + g \right) \quad (2)$$

where $\mathrm{K}(\Psi_m)$ represents the hydraulic conductivity as a function of matric potential (Ψ_m, KPa), which is 0.00019 kg s m^{-3} for silty loam soils (Villalobos et al., 2016), z (m) is the vertical distance among two soil depths, g (m s^{-2}) is the gravitational acceleration.

2.2. Experiment 2 – potted apple trees

2.2.1. Experimental design

Four apple trees (cv. Golden Delicious, rootstock M9, 3-years old) in 8 L pots filled with an organic substrate were transferred at the beginning of June 2020 in an area covered with a transparent shelter, to protect them from precipitation. During the preliminary phase of the experiment (two weeks), trees were regularly irrigated with local tap water ($\delta^2H = -80.8 \pm 0.4‰$).

The experiment started on June 23, 2020, at 10 PM, with the addition of ^2H-enriched water. The enriched solution was prepared in a single tank just before the experiment ($\delta^2H = 1550 \pm 18‰$). After a thorough homogenization, 1.5 L of labeled water were applied - to the pots using a rain-shower watering cans. After the irrigation, the soil in each pot was covered with a plastic film to avoid evaporation from the soil surface. Pots were lifted from the ground using a metal ring and percolating water was collected in pot dishes. The following day, June 24, was sunny (11 h of sunshine) with maximum temperatures above 30 °C and ca. 50% relative humidity.

2.2.2. Potted tree sampling

Before pot irrigation, a soil sample was collected from each pot. Percolated water (on average 0.5 ± 0.1 L) was taken from each pot dish at the end of percolation (ca. 30 min after irrigation). Tree samplings were scheduled before the irrigation (0 h) and 6, 10, 14, 18, and 30 h after the water supply. At each sampling, a single shoot (min. 20 cm length) per plant was chosen, and two fully expanded apical leaves and the shoot axis (without bark, differently from Experiment 1) were collected. At the end of the experiment, soil cores were collected from each pot to obtain a representative subsample. All the samples were directly transferred into airtight glass vials, with a screw cap and rubber septum, sealed and stored frozen until processing.

Before each sampling, the pot weight was recorded to estimate tree transpiration. The water content of leaf, shoot axis, and soil samples was determined gravimetrically, as previously described for Experiment 1 (Section 2.1.3).

2.3. Cryogenic vacuum distillation

Cryogenic vacuum distillation (CVD) was applied to recover water from soil and tree samples collected during Experiment 1 and 2 following the method described by Koeniger et al. (2011) and reported by Beyer et al. (2018) and Millar et al. (2018) with slight modifications.

The vials containing the frozen samples were connected to empty vials, then vacuum sealed through stainless steel needles. The filled vials were then placed in a thermoblock, heated through a hot plate (200 °C, 15 min), while the empty vials were immersed in liquid nitrogen. The distilled water was transferred into 2 mL vials and stored in the refrigerator until analysis. Extraction efficiency was estimated comparing the sample weight after CVD and subsequent oven drying (105 °C, 24 h). Overall, the extraction efficiency was > 99%, in agreement with other studies (Millar et al., 2018; Tsuruta et al., 2019; Wu et al., 2019). Such an extraction efficiency is high enough to prevent artifacts due to water isotope fractionation (Araguás-Araguás et al., 1995).

2.4. Laboratory isotope analysis

The isotopic composition (δ^2H) of water samples (^2H-enriched water, irrigation water, rainwater, groundwater) and water extracts from soil samples was measured through cavity ring-down spectroscopy (CRDS L2130-*i*, Picarro Inc.). The instrument is equipped with a vaporizer unit for liquid water injection (vaporization module A0211, Picarro Inc.) and an autosampler (A0325, Picarro Inc.). Injection volume was set at 1.8 μl, sucked through a 10 μl syringe. Ten injections were performed for the in-house water standards (calibrated against VSMOW and SLAP certified reference materials) and seven for the water samples not subject to ^2H enrichment. In analytical sequences including samples for which an artificial ^2H enrichment was expected, the number of injections was increased to 15 and 12 for standards and samples, respectively. Standards were measured repeatedly, at the beginning, at the end, and after blocks of 8–10 samples.

To deal with memory effect (sample-to-sample memory), the first three (for the water samples not subject to ^2H enrichment) or five (for the ^2H-enriched samples) measurements per sample were removed before averaging the ratios (Gröning, 2018; Penna et al., 2012). Results were processed using the Picarro's ChemCorrect post-processing software package to identify samples affected by spectral interference of organic compounds. Heavy contamination was detected in less than 3% of the soil extracts. The isotopic ratios of these samples were excluded from the data analysis.

The δ^2H of plant water extracts (shoot axis and leaf samples), in addition to all the samples from Experiment 2, was determined with a Gas Bench II (Thermo Scientific) coupled to a Continuous Flow Isotopic Ratio Mass Spectrometer (CF-IRMS, Delta V Advantage Conflo IV, Thermo Scientific), due to the high organic content that would have interfered with the CRDS analysis. The methodology with the Gas Bench II foresees that 0.2 mL of sample is added to a vial and subsequently the headspace flushed with an equilibration gas (2% H_2 in helium). A platinum stick was added to the vials as the catalyst for the equilibration phase. After the required equilibration time (40 min) the headspace was analyzed with the IRMS. Standards and blanks were analyzed within each sequence at the beginning, at the end, and after each block of 8–10 samples. The number of injections was set to eight, and the average per sample was calculated based on five injections.

Isotopic ratios were expressed relative to the VSMOW international standard (Vienna Standard Mean Ocean Water) in per mil notation (‰) (i.e. isotopic composition):

$$\delta^2H(‰) = \left(\frac{R_{sample}}{R_{standard}} - 1\right) \cdot 1000 \quad (3)$$

where R_{sample} and $R_{standard}$ represent the heavy to light isotope ratios ($^2H/^1H$) of the sample and the standard, respectively.

Instrumental long-term precision for CRDS and IRMS were evaluated throughout the measuring period analyzing the in-house water standards. The precision, expressed as twice the standard deviation of multiple injections, was 1.04‰ for the CRDS and < 3.0‰ for the IRMS, in line with other studies (Beyer et al., 2018, 2016; Millar et al., 2018). According to Beyer et al., (2016, 2018), for ^2H-artificially enriched samples, the standard deviation can be up to five times higher. Our data are in agreement with this observation, as the standard deviation of control samples was 0.27‰ while that of enriched samples was 1.13‰, on average. The comparison between the CRDS and IRMS isotope ratio measurements performed on a set of water samples not subject to organic contamination, reported in detail in a previous study (Penna et al., 2021), showed only a negligible difference, close to the instrumental precision, between the measurements performed by the two instruments (Maruyama and Tada, 2014; Wassenaar et al., 2012).

2.5. Assessment of the water sources in soil and tree samples

A two-component mixing model was applied to quantify the fraction of ^2H-enriched irrigation water present in soil (Eq. 4) and shoots (Eq. 5) during the experiments. For soil water, the underlying assumption was that sampled soil water was a mixture of pre-irrigation soil water (considered to have the same isotopic composition of the soil water in the control plot) and irrigation water. Analogously, for shoot water, the assumption was that the sampled shoot water was a mixture of pre-irrigation shoot water (considered to have the same isotopic composition than shoot water in the control trees) and irrigation water. The two components sum up to 100% of water in the soil or shoot sample. Based on these assumptions, the mixing model was applied as follows:

$$f_{IW\ in\ \ soil} = \frac{\delta^2 H_{irrigated\ soil} - \delta^2 H_{control\ soil}}{\delta^2 H_{IW} - \delta^2 H_{control\ soil}} \quad (4)$$

$$f_{IW\ in\ shoots} = \frac{\delta^2 H_{irrigated\ tree} - \delta^2 H_{control\ tree}}{\delta^2 H_{IW} - \delta^2 H_{control\ tree}} \quad (5)$$

Where f is the fractional contribution of irrigation water (*IW*) in the water sampled from the soil (Eq. 4) or shoot (Eq. 5) in the irrigated plots, δ^2H of irrigated and control plots represents the isotopic composition of the soil (Eq. 4) or shoot (Eq. 5) water sampled in the irrigated or control plots, respectively. The uncertainty of the mixing models was calculated according to Genereux (1998) at 95% confidence. For each component, the uncertainty used to calculate the overall model uncertainty corresponded to the standard deviation of the multiple injections for each water extract (through IRMS or CRDS) multiplied by the corresponding critical value of the Student's t-distribution (two tails, 95% confidence).

Another mixing model was performed to quantify the fraction of leaf and shoot axis water derived from soil water taken up by the trees during the experiment. For this purpose, we considered only the 0–0.6 m soil layer, as its ^{2}H signature was significantly affected by the labeling procedure. The underlying assumption was that shoot water after irrigation was a mixture of pre-event water (corresponding to water in control soil) and soil water present in the 0–0.6 m layer after irrigation, and the sum of the two components in the shoots was 100%. The following equations were applied for shoot axes and leaves, respectively:

$$f_{SW\ in\ \ shoot\ axes} = \frac{\delta^2 H_{irrigated\ tree} - \delta^2 H_{control\ soil}}{\delta^2 H_{irrigated\ soil} - \delta^2 H_{control\ soil}} \quad (6)$$

$$f_{SW\ in\ leaves} = \frac{\delta^2 H_{irrigated\ tree} - \delta^2 H_{control\ \ tree}}{\delta^2 H_{irrigated\ soil} - \delta^2 H_{control\ tree}} \quad (7)$$

Where f is the fractional contribution of soil water (*SW*) to tree water, δ^2H$_{\text{irrigated tree}}$ and δ^2H$_{\text{control tree}}$ represent the isotopic composition of water in shoot axes or leaves, and ^{2}H$_{\text{irrigated soil}}$ and ^{2}H$_{\text{control soil}}$ the weighted isotopic composition of soil water at 0–0.6 m depth, calculated considering the water content and the ^{2}H enrichment of each soil layer. Due to fractionation processes related to transpiration, leaf water is typically more enriched in ^{2}H compared to shoot axis water (Benettin et al., 2021; Beyer et al., 2016). Applying Eq. (7) instead of Eq. (6) for leaves, and hence subtracting the ^{2}H abundance in control leaves to irrigated leaves, we excluded the attribution of this enrichment to a fraction of artificially-enriched water absorbed from the 0–0.6 m soil layer. The uncertainty of the mixing models was calculated as described above for Eq. (4) and Eq. (5).

A two-component mixing model was also applied to data from Experiment 2 to determine the isotopic composition of soil water (SW) at the end of the experiment, given the isotopic composition of pre-irrigation soil water (pre-SW), and the ^{2}H-enriched irrigation water (IW). The underlying assumption was that soil water was a mixture of pre-irrigation soil water and irrigation water and that the sum of the two components in the soil was 100%. The model was applied according to the following equation:

$$f_{IW\ in\ \ soil} = \frac{\delta^2 H_{SW} - \delta^2 H_{pre-SW}}{\delta^2 H_{IW} - \delta^2 H_{pre-SW}} \quad (8)$$

To calculate the fractional contribution of soil water (SW) to shoot water ($f_{\text{SW in shoots}}$) at each sampling, we applied Eq. (6) and Eq. (7) comparing the isotopic composition of shoot and soil samples at the beginning (0 h) with that measured at each sampling time.

2.6. Statistical analysis

Results are reported as mean ± standard deviation (1 sd). Applying the interquartile method, outliers were identified and removed from the dataset. T-test and ANOVA with Tukey HSD post-hoc test were applied to identify significant differences among groups (control vs. irrigated samples, different soil layers, sampling days), on normally distributed and homoscedastic data. If the conditions to apply parametric tests were not fulfilled, non-parametric tests were applied (Wilcoxon test instead of t-test, Kruskal-Wallis test instead of ANOVA). When longitudinal data were compared, namely data referred to the same sample over time, a linear mixed model was applied. The significance level was set at 0.05. The statistical analysis was carried out using the computing environment R version 4.0.3 (R Core Team, 2020).

3. Results

3.1. Experiment 1 – field-grown apple trees

3.1.1. Soil water dynamic

The groundwater table depth ranged between 0.9 and 1.0 m from the ground surface in the first days of the experiment (July 23–26, 2019) and, subsequently, it reached 0.84 m during the last sampling days in response to a rainfall event that occurred on July 26–27, 2019 (Supplementary Table S1).

Fig. 2 reports soil water content at the first and final sampling (2 and 168 h after irrigation), measured at different depths in the control and irrigated plot. In both plots, soil water content decreased moving from the top layer to 0.4–0.6 m depth and then increased again down to 0.8 m depth (Fig. 2). Two hours after the irrigation, the highest difference in water content between the control and irrigated plot was measured in the shallowest soil layer (upper 0.1 m depth, 49.5 ± 1.8% and 43.0 ± 1.6% respectively). Significant differences were measured also between 0.2 and 0.4 m depth, with higher water content in the irrigated plot between 0.2 and 0.3 m depth and an opposite trend in the following layer. In general, a gradual decrease of soil water content occurred from the top layer to depth of 0.4–0.5 m, where it reached its minimum value (29%). At depth between 0.3 and 0.7 m, soil water content was rather stable (31.1 ± 2.0%), but it increased in the deepest investigated soil layer (0.7–0.8 m, 37.2 ± 2.6%). In the subsequent samplings no significant variation in the soil water content at different depths and between irrigated and control plots was observed (Supplementary Fig. S1).

Applying soil moisture-derived values of soil water potential and the soil physical properties (Eq. 1), the estimated values of water flow from the groundwater table to 0.7 m and 0.6 m depth were 12.1 and 3.7 mm day^{-1}, respectively (Eq. 2). The capillary rise to soil layers above 0.6 m was, on the contrary, negligible.

Fig. 3 reports the average δ^2H of soil water extracts collected from the irrigated and control plots, at the beginning (2 h, upper panel) and the end (168 h, lower panel) of the experiment. In the control soil, moving from the topsoil to 0.8 m depth, the values of δ^2H constantly decreased towards more depleted values, from − 55.9 ± 6.1‰ at 0.1 m depth to − 87.5 ± 1.4‰ at 0.7–0.8 m depth, on average. The water extracted from the deepest soil layer (0.7–0.8 m depth) showed an isotope composition similar to that of groundwater (δ^2H = −89.6 ± 1.0‰) collected from the piezometer. No significant change of δ^2H was recorded in the control soil during the experiment, indicating no lateral water movement from the adjacent irrigated plots.

The ^{2}H enrichment after irrigation was particularly marked in the upper soil layer (0.1 m depth). The maximum enrichment in this layer was measured 2 h after irrigation (847 ± 180‰), while in the following days the measured ratio decreased and settled down to lower but still highly enriched values (748 ± 282‰, 611 ± 252‰, and 635 ± 49‰ after 24, 48, and 168 h from irrigation, respectively). The decrease in the ratio of the first layer was followed by an increase of the ratio in the subsequent layers, as mobile water slowly penetrated in depth. For instance, the second soil layer (0.1–0.2 m) had a δ^2H equals to 89 ± 58‰ at the first sampling (2 h after irrigation), it increased to 421 ± 280‰ the following day, and then it settled down around 262 ± 108‰ at the last sampling. The δ^2H measured in the subsequent layers showed a similar trend, with a lower increment at increasing sampling

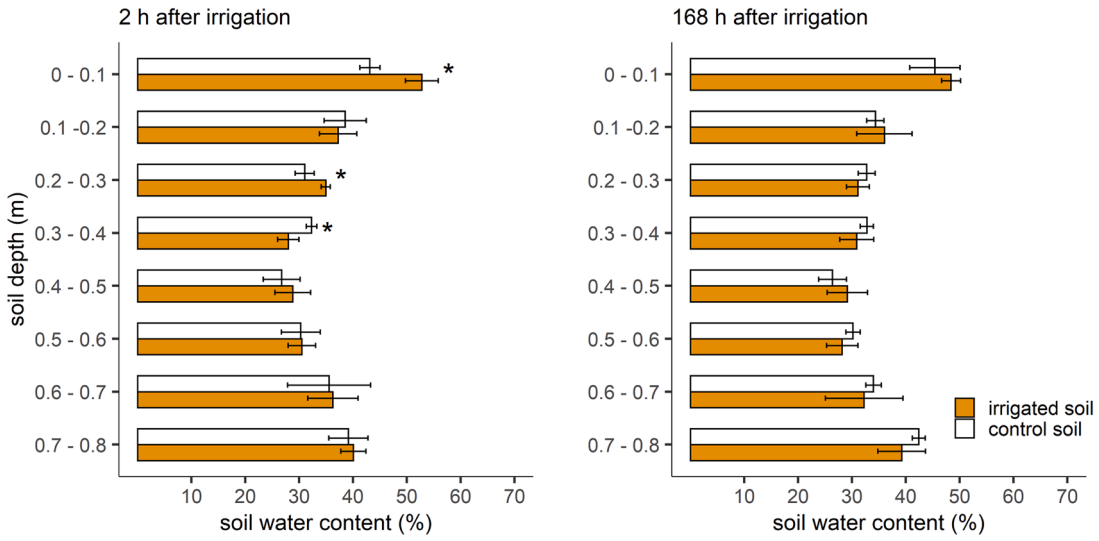

Fig. 2. Experiment 1. Gravimetric soil water content measured in control and irrigated plots at different depths, 2 h (left panel) and 168 h (right panel) after irrigation. Each bar represents the mean ± sd of the layer. Asterisks denote significant differences between control and irrigated plot.

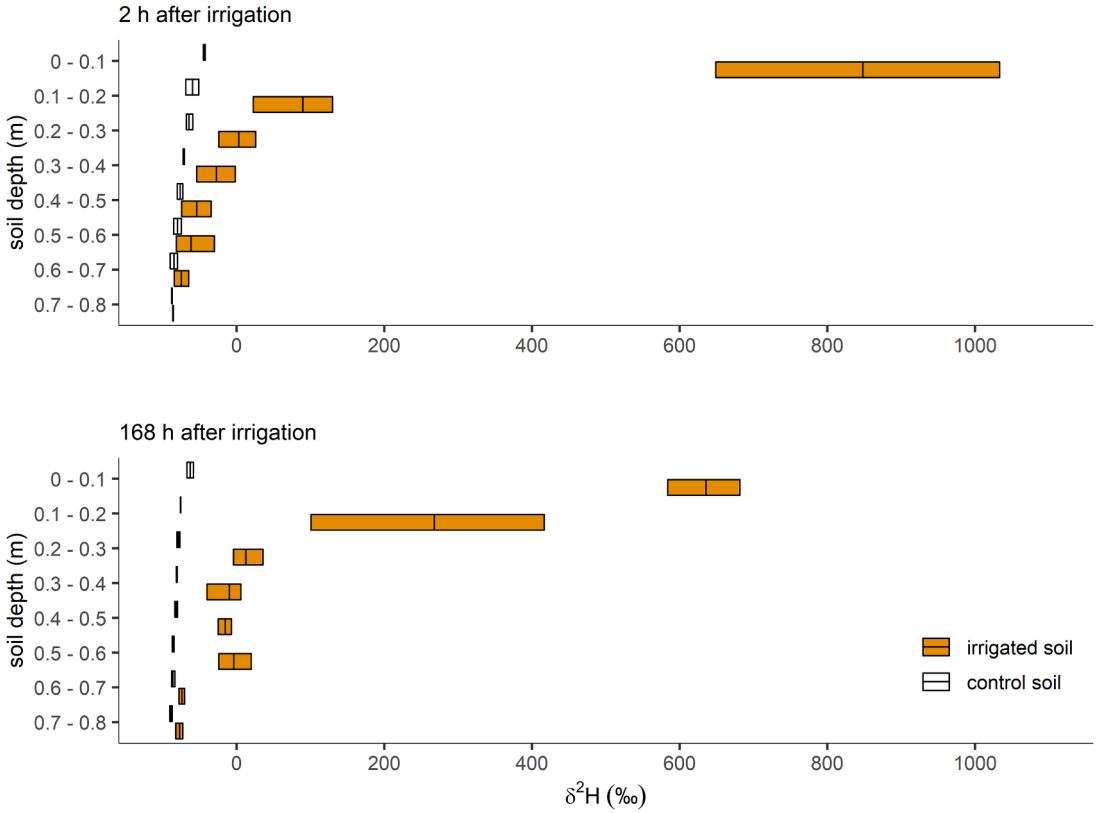

Fig. 3. Experiment 1. Comparison of δ^2H in control (C) and irrigated (I) soil water extracts at each depth for the first (2 h, upper panel) and the last (168 h, lower panel) soil sampling. Each floating bar represents min to max δ values and the vertical line the mean.

depth (Supplementary Fig. S2). The lowest δ^2H variation was measured in the deepest soil layers (0.6–0.8 m), where a not significant increment was measured in the isotopic composition of soil water of the irrigated plots compared to that of the control plots (−58 ± 25‰ and −87 ± 2‰, respectively). No significant change in soil moisture or isotopic composition was registered following field irrigation (20 mm, −98.8‰) and rainfall events (19 mm, −40.2‰), hence their impact on our experiment was very likely negligible.

Following Eq. (4), the fraction of soil water derived from ^{2}H-enriched irrigation water was estimated (Fig. 4). In agreement with the enrichment measured in the different soil layers, the contribution sharply decreased from 0 to 0.1–0.1–0.2 m, where it represented 54–43% and 9–18% of the total water at 2 h and 168 h after irrigation, respectively. The contribution of irrigation water in the soil layer at 0.2–0.6 m depth was significantly lower and constant, between 1% and 4% and 4–5% of the total water at 2 h and 168 h after irrigation, respectively. In general, the deepest layer (0.6–0.8 m depth) did not show a significant presence of irrigation water (Fig. 4). A complete overview of the contribution of

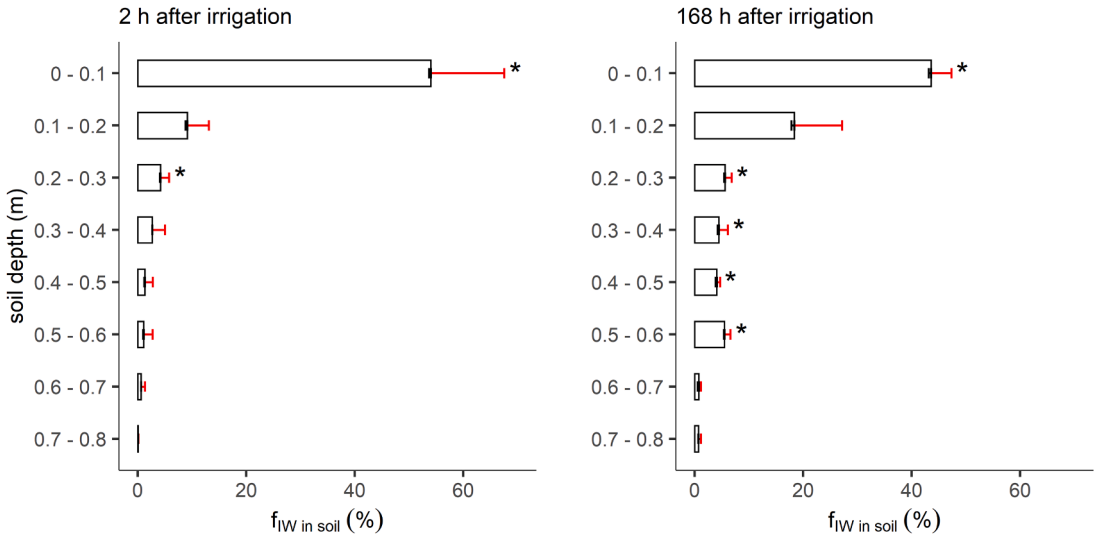

Fig. 4. Experiment 1. Percentage contribution of irrigation water to soil water (irrigated plots) as calculated applying a two-component mixing model (Eq. 4) 2 h (left panel) and 168 h (right panel) after irrigation. Each bar represents the mean value of the four irrigation plots. Error bars indicate the standard deviation (red error bar) and the uncertainty of the model (black error bar) calculated according to Genereux (1998). Asterisks denote mean values that are statistically different from zero, considering a 95% confidence interval.

irrigation water, including intermediate samplings, is reported in Supplementary Fig. S3. On average, the applied irrigation water in the 0–0.6 m soil layer at the first and last sampling was respectively ca. 12% and 14% of the total soil water.

3.1.2. *Tree water uptake*

Within the experimental period, ET_0 was on average 3.25 mm day^{-1}. ET_0 was highest in the first two days (5 mm day^{-1}), then it decreased. The lowest value was recorded 5 days after irrigation (1 mm day^{-1}), on a rainy day. After this event, ET_0 raised again to pre-rain values (3.8 mm day^{-1}, on average). Daily ET_0 data are reported in Supplementary Table S1.

On the last sampling occasion, control and irrigated trees had a similar total water content; average values recorded in leaves and shoot axes were 65.1 ± 1.3% and 56.7 ± 1.2% (on fresh weight), respectively.

The isotopic composition of the extracted water from leaf and shoot axis samples is shown in Fig. 5. In control trees, transpiring leaves were more enriched in ^{2}H than shoot axes (δ^2H on average −9.9 ± 5.7‰ and −72.1 ± 5.6‰, respectively), with no difference given by the sampling position. As observed in control trees, leaves of the irrigated trees had a significantly higher δ^2H than that of shoot axes when sampled at 2 h after irrigation. At this sampling time, irrigated and control trees had similar δ^2H in both organs (Fig. 5). The following samplings highlighted a gradual but significant increase of δ^2H in both shoot axes and leaves until reaching a plateau. No significant difference was observed comparing samples collected at the bottom and top of the canopy. The δ^2H of the shoot axes increased within the first 24 h after the water supply and then remained steady for the entire experimental period (53.9 ± 10.8‰). The leaf δ^2H steadily increased until 8 h after the water supply and then leveled off (43.2 ± 8.0‰), with the only exception of the sampling at 72 h, significantly lower.

The application of the two-component mixing model (Eq. 5) returned

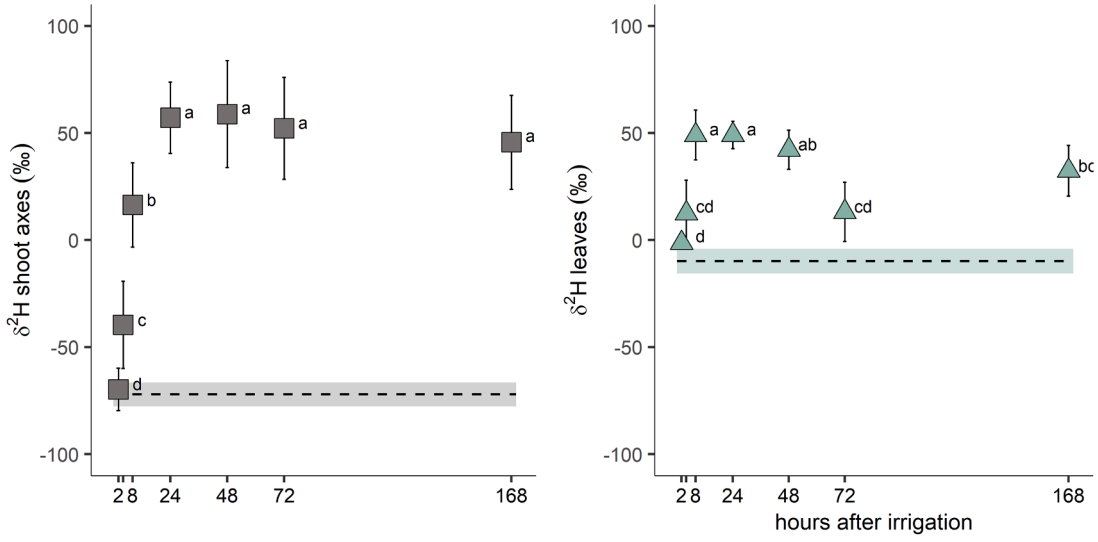

Fig. 5. Experiment 1. δ^2H in shoot axes (left panel) and leaves (right panel) collected at different times after irrigation, in irrigated trees. Each point represents the mean ± sd of the four trees and the two sampling positions (bottom and top part of the canopy). The shaded bands represent the average composition (± 1 sd) of control shoot axes and leaves, and the dotted line is the average δ value of control samples. Different letters indicate statistically significant differences and points with no common letters are significantly different.

the fraction of shoot axis and leaf water deriving from irrigation water reported in Fig. 6. Irrigation water fractions were larger in the shoot axes than in the leaves. When the δ^2H of tree samples reached a plateau (Fig. 5), the amount of water coming from irrigation water was 7.8 ± 0.4% for the shoot axes and 3.3 ± 0.5% for the leaves (excluding the lowest value at 72 h after irrigation). Considering both the temporal and spatial data variability, this was comparable to the estimated model uncertainty (Fig. 6).

Considering that irrigation water infiltrated in the soil and mixed with the soil water already present before irrigation, the fraction of ^{2}H present in the tree samples that derived from soil water was estimated applying Eqs. 6 and 7 (Fig. 7). As discussed above, ^{2}H-enriched irrigation water infiltrated in the soil down to 0.6 m (Fig. 4), hence the calculation was limited to the 0–0.6 m soil layer. Two hours after irrigation, the contribution of soil water in tree samples was less than 5%, but it increased to 10–15% at 4 h after irrigation. When the δ^2H of tree samples reached a plateau (after 8 h for the leaves and 24 h for the shoot axes, as reported in Fig. 5), the calculated water fraction coming from the enriched soil layer was on average 48 ± 3% for the shoot axes and 26 ± 2% for the leaves. Such a contribution dropped at 72 h leaf sampling (14%). Despite a large data variability among the four irrigated trees, indicated by the red vertical lines in Fig. 7, the contribution of soil water to shoot axes and leaf water was constant between 24 and 168 h after irrigation, with a rather low estimated model uncertainty.

3.2. Experiment 2 – potted apple trees

3.2.1. Transpiration and shoot water content

Cumulative tree transpiration, expressed as kg of water lost during the experiment, for the different sampling times is reported in Fig. 8. As expected, the highest water loss occurred between 8 AM and 4 PM. On average, ca. 85% of the irrigation water retained by the soil after irrigation was lost in 30 h by trees through transpiration. Nonetheless, the gravimetric water content at the end of the experiment was still high (195 ± 10%), due to the large water holding capacity of the organic substrate. The water content of leaves was higher than that of shoot axes (without bark) (Supplementary Table S3), in agreement with Experiment 1, and showed an expected pattern related to the sampling time and tree transpiration, with the highest water contents during the night.

3.2.2. Soil and tree water isotopic composition

Percolated water was a mixture of both pre-irrigation soil water and ^{2}H-enriched irrigation water, as indicated by the average δ^2H value (644 ± 277‰). The variability of the isotopic composition of percolated water among pots was likely related to differences in soil moisture before the irrigation with ^{2}H-enriched water.

The δ^2H of soil water measured at the end of the experiment was quite homogeneous among trees (712 ± 51‰), and showed a high enrichment compared to the pre-irrigation soil water (−79.9 ± 1.3‰). The enrichment obtained for soil water attested that pre-irrigation soil water was still present in the soil and the proportion between the two water sources was similar. Irrigation water contributed to ca. 50% of total soil water extracted with CVD (Eq. 8).

The isotopic composition of tree samples at the different sampling times is summarized in Fig. 8. The leaf transpiration explains the isotopic composition of leaf samples being more enriched compared to shoot axes before the addition of labeled water (−24 ± 5‰, on average). As observed in Experiment 1, the presence of labeled water in leaf samples significantly differed from that in shoot axes. Water extracts from the shoot axes (without bark) and leaves did not show the presence of labeled water at the pre-dawn sampling of 4 AM (6 h after the water supply), providing no evidence of significant water uptake and transport to the canopy by root pressure during the night. The delta ratios slightly increased 10 h after the irrigation cycle (8 AM), although they were not significantly different from the previous sampling. Between 10 and 14 h after irrigation (from 8 AM to 12 PM), the δ^2H values of both shoot axes and leaves steeply increased and such increase continued until 4 PM, then it leveled off, showing final values of 401 ± 21‰ and 242 ± 26‰ at the last shoot axis and leaf sampling (30 h), respectively. The increase of δ^2H values in both shoot axes and leaves matched the tree transpiration rate (Fig. 8). The isotopic composition of tree samples was significantly lower compared to that of soil water at the end of the experiment (δ^2H =712 ± 51‰).

Table 2 summarizes the soil water contribution to shoot water (shoot axes and leaves), estimated by Eqs. 6 and 7. In agreement with the lack of transpiration during the night, there was no contribution of soil water to shoot water at the first two samplings after irrigation. At the last sampling (30 h after irrigation), 61 ± 3% and 36 ± 4% of the total water present in shoot axes and leaves was derived from root absorption. The contribution of soil water uptake to total shoot axis and leaf water in Experiment 2 (using both data at 18 and 30 h from the water supply,

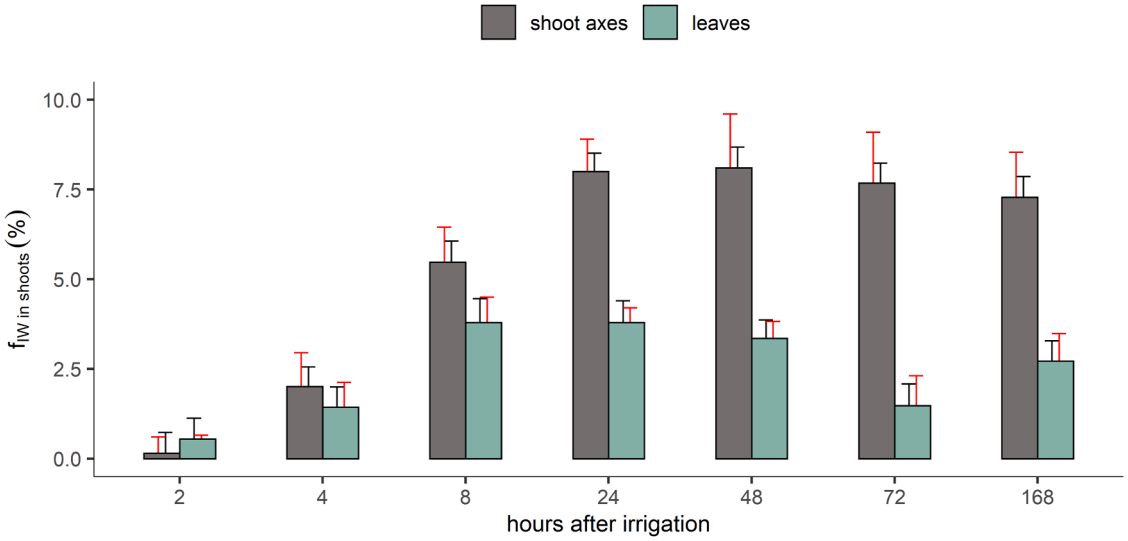

Fig. 6. Experiment 1. Fractional contribution of irrigation water (IW) to shoot axis and leaf water (Eq. 5). Data are reported as percentages. Bars correspond to the average values of the four irrigated trees and the two sampling positions (bottom and top part of the canopy). Error bars indicate the standard deviation (in red) and the uncertainty of the model (in black) calculated according to Genereux (1998).

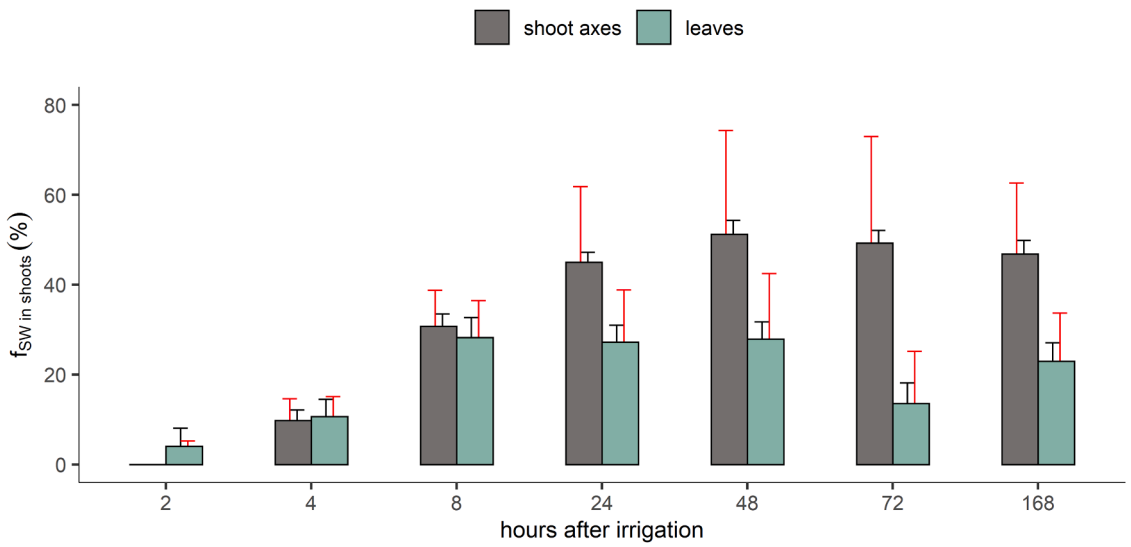

Fig. 7. Experiment 1. Fractional contribution of soil water from the 0–0.6 m soil layer to shoot axis and leaf water, calculated applying Eq. (6) and Eq. (7), respectively. Data are reported as percentages. Bars correspond to the average values for the four irrigated trees and the two sampling positions (bottom and top part of the canopy). Error bars indicate the standard deviation (red error bar) and the uncertainty of the model (black error bar) calculated according to Genereux (1998).

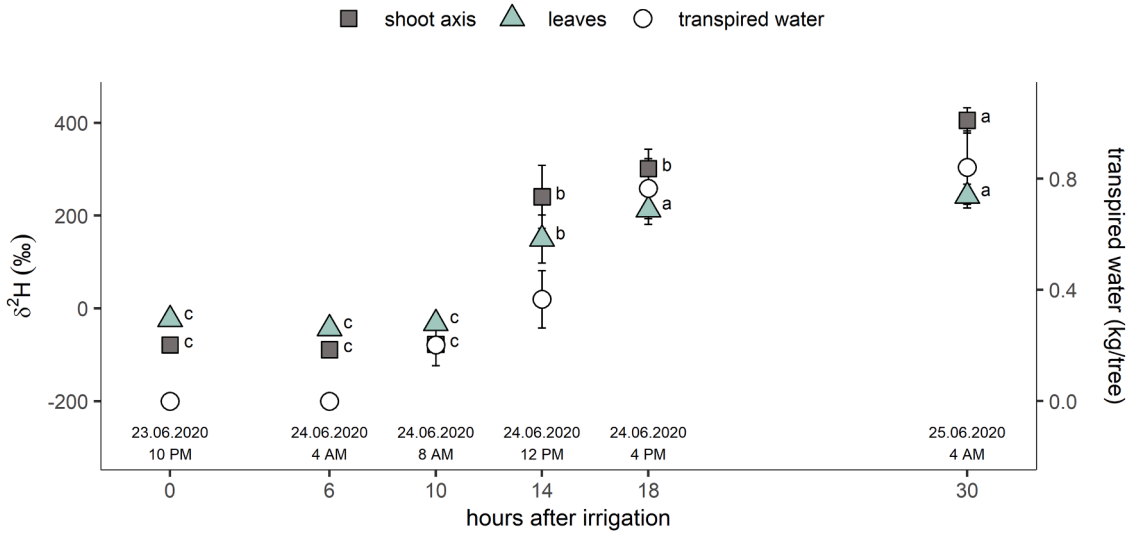

Fig. 8. Experiment 2. Isotope composition of tree samples at the different sampling times (left axis). On the right axis, the average cumulative amount of transpired water per pot at each sampling since the irrigation event (hours = 0) is reported. Points represent average values and bars the standard deviation of the four trees (covered by symbols for the first points). Letters after symbols indicate significant differences of δ^2H between samplings for each organ.

Table 2
Experiment 2. Contribution (%) of soil water to shoot water, calculated applying Eq. (6) and Eq. (7). Data are reported as mean ± sd.

Hours after irrigation	Time of sampling	$f_{SW\ in\ shoot\ axes}$	$f_{SW\ in\ leaves}$
6	4 AM	-1.2 ± 0.4%	-2.6 ± 1.6%
10	8 AM	0.2 ± 1.5%	-1.1 ± 2.6%
14	12 AM	40.2 ± 6.8%	23.4 ± 6.3%
18	4 PM	48.4 ± 7.0%	32.4 ± 6.2%
30	4 AM	61.4 ± 3.3%	36.2 ± 3.6%

Table 2) did not significantly differ from that quantified in Experiment 1 (using data at 24 h, Fig. 7) according to a t-test for independent samples.

4. Discussion

4.1. Soil water dynamics

Root density data for the analyzed orchard indicate that about half of the fine root biomass was concentrated in the upper 0–0.2 m soil layer and that more than 90% of the fine roots was present in the 0–0.6 m soil layer (Penna et al., 2021). Soil moisture measured in control and irrigated samples during the experimental period was similar, despite the lack of irrigation in the control plot. Based on soil moisture data, we were not able to detect a temporal decrease in soil moisture caused by tree transpiration, likely due to the different positions where samples were taken on each sampling time. On average, soil moisture was highest in the upper as well in the deepest soil layers, whereas the lowest

values were observed at a soil depth of 0.4–0.5 m in both control and irrigated plots. The presence of the impermeable plastic cover on the soil surface most likely limited water evaporation from the soil surface, maintaining high levels of soil moisture in the upper layer (Zheng et al., 2017). Even the lowest soil moisture values measured at depth of 0.4–0.5 m, were on average higher than 30%, suggesting that roots did not experience any water stress during the experiment. The inversion in soil water content towards higher values measured in the deepest soil layers can be related to the presence of the groundwater table at ca. 0.9 m depth. Data for a soil texture comparable to our case and with groundwater depths between 0.8 and 1 m reported possible upward flow rates up to 5–6 mm day^{-1} but only up to 0.6 m depth (Doorenbos and Pruitt, 1977), similar to the values of maximum capillary rise that we estimated (12.1 and 3.7 mm day^{-1} at 0.7 and 0.6 m depth, respectively). Our findings support the results of the study conducted by Penna et al. (2021) in the same area, who compared soil measurements at two depths (0.25 and 0.5 m depth) and reported constantly higher water content and more depleted isotope signals in the deeper soil layer in the orchard with the shallower groundwater table (same orchard of our study), suggesting a possible groundwater contribution to soil water recharge at these depths. The presence of a small portion of fine roots below 0.6 m depth and the relatively high soil water content at 0.6–0.8 m depth justifies the hypothesis that part of tree water might derive from the groundwater table.

We found a rather high variability of labeled soil water values among different irrigation plots (Figs. 3 and 4), which might be due to the soil sampling procedure (single soil core at each sampling) and to an uneven soil infiltration pattern (Clothier et al., 2007; Gazis and Feng, 2004; Zhang et al., 2018). The effect of this variability was also propagated to the results of the mixing models that we applied to estimate the fraction of soil water absorbed by the trees and present in the shoots. Indeed, results obtained applying the mixing models (Eqs. 6 and 7) showed a rather high variability considering the independent experimental units, while the goodness of the model itself was rather high, as indicated by the low estimated uncertainty (Fig. 7). This means that our estimations suffered more from soil spatial heterogeneity rather than from analytical factors related to isotope ratio measurements (Beyer and Penna, 2021).

A key point of soil water studies is the choice of soil water recovering techniques to collect a water pool that is representative of the soil water bioavailable for root uptake. As reported in numerous studies (Di Bonito et al., 2008; Orlowski et al., 2016a, 2016b), soil water extraction represents a critical step of the procedure: applying different techniques often involves a different water extraction capacity, affected also by the soil type (Orlowski et al., 2016b; Tsuruta et al., 2019). Cryogenic extraction allows the recovery of the whole amount of water present in the soil. Only a fraction of this water can be effectively absorbed by roots, depending on the potential gradient applied by plants, with water held by the soil at low potentials being inaccessible for plants. Moreover, interactions between mobile, bound, and tightly bound water in soil are difficult to quantify and variable depending on soil physical properties (Adams et al., 2020; Sprenger et al., 2019; Thielemann et al., 2019; Vargas et al., 2017).

Based on soil water isotopic composition 2 h after irrigation, most of the water was found in the first 0.2 m of soil. In the following days, irrigation water penetrated to deeper soil layers, to a maximum of 0.6 m depth (Supplementary Fig. S2 and S3), and mixed with pre-irrigation soil water. Such mixing occurred with different intensities along the profile, but no significant enrichment was measured below 0.6 m depth (Fig. 4). Despite water movements between topsoil and deeper layers, irrigation water represented ca. 12–18% of the total soil water present to 0.6 m depth during the experimental period (Fig. 4 and Supplementary Fig. S3). Considering that no more water was added to the experimental units after the irrigation with ^{2}H-enriched water and that the soil cover prevented evaporation from the surface, a stable condition was established in the soil-tree system during the field experiment.

4.2. Water uptake dynamics by field-grown apple trees

Soil and leaf water content suggests an adequate water availability for tree requirement in both the irrigated and the control plots during Experiment 1. The summer climate at this Alpine site is also relatively mild with ET_0 values not particularly high (Supplementary Table S1) compared to apple production areas at lower elevation in the same region (Montagnani et al., 2018; Zanotelli et al., 2019, 2022).

Analyzing the tree water isotopic composition, we were able to delineate more precisely the dynamics of water uptake. Trees were irrigated at 9 AM on a sunny summer day when tree transpiration was already ongoing. As reported in Fig. 5, a slight increase in the water δ^2H (compared to the control trees) extracted both from shoot axes and the leaves was already visible after 2 h, but it was more evident at the 4 h sampling, indicating a rapid uptake of the irrigation water soon after its distribution. The fact that fine root density was highest in the upper 0–0.2 m soil layer might have contributed to the rapid uptake of labeled water. The time lag between the irrigation water supply and the presence of irrigation water in the tree transpiring organs is of practical importance in irrigation management. Although irrigation water might only represent a relatively low fraction of total leaf water, its rapid transport from roots to the leaves could allow the recovery from drought stress conditions.

Within the first sampling day, shoot isotopic composition continued to increase, showing a progressively higher contribution of irrigation water to shoot water (Fig. 5, Fig. 6, and Fig. 7), following the transpiration-driven root water uptake. Interestingly, shoot isotopic composition reached a plateau and remained rather constant from 24 h after irrigation to the end of the experiment, without showing any additional significant increase in both leaves and shoot axes in the following six days, except for leaves at 72 h from irrigation. The low isotopic composition of leaf samples at this sampling point might have been determined by the low transpiration rate registered on that day (Farquhar et al., 2007; Gan et al., 2002; Sheshshayee et al., 2005). Additionally, the night before this sampling, trees were irrigated by an overhead sprinkler (roughly 20 mm). We hypothesized that part of the irrigation water (δ^2H = −98.8‰) fallen on the leaf surface might have been absorbed (foliar water uptake) (Berry et al., 2019; Schreel and Steppe, 2020), determining a decrease in the leaf isotopic composition. Similarly to what was observed in the field experiment, the ^{2}H abundance in potted trees sharply increased from 8 AM to 12 PM, but then it tended to level off at the two successive sampling occasions, following a trend similar to transpiration rate (Fig. 8). Seeger and Weiler (2021), who collected xylem sap at different heights from the stem of 90–100 year-old *Fagus sylvatica* L. trees after the application of labeled water to the soil, also found that tree isotopic composition gradually increased until reaching a plateau approximately 6–14 days after water distribution; such a delay with respect to our experiment might be explained by the different size of the trees.

Both shoot axes and leaves were characterized by a significantly lower isotopic composition (with maximum δ-value around 50–60‰) compared to that of soil water. The estimated fraction of irrigation water present in the shoot axes and leaves was 7.8 ± 0.4% and 3.3 ± 0.5% of the total water, respectively. Applying Eqs. 6 and 7, we estimated that the maximum contribution of the water taken from the ^{2}H-enriched soil layer (0–0.6 m depth) to total plant water was 48 ± 3% and 26 ± 2% in shoot axes and leaves, respectively (Fig. 7). Based on these results, a significant water fraction did not derive from the soil layer where irrigation water had infiltrated. Similar results were obtained by Rowland et al. (2008), who applied ^{2}H-enriched irrigation water to evaluate water use in a peanut cultivation: applying a two-component mixing model, they calculated that the fraction of irrigation water present in the peanut stem (collected through CVD) was ca. 40%, but they did not discuss the origin of the remaining water fraction.

4.3. Origin of the shoot water

To explain the limited fraction of shoot water deriving from the 0–0.6 m soil depth during the experimental period, we put forward two possible explanations:

1. trees absorbed a significant amount of water in the deeper soil layer (0.6–0.8 m depth) that had not been significantly enriched by labeled water;
2. a significant fraction of the cryogenically-extracted shoot water was already present before the starting of the experiment (pre-event water) and it mixed at very low rates with the recently absorbed labeled water.

The first explanation would be plausible if a large part of the root system developed below 0.6 m depth, as it happens when vigorous apple rootstocks are used (Song et al., 2018). In our experiment, however, trees were grafted on the dwarfing M9 rootstock and most of the roots were located in the 0–0.6 m soil layer, as reported for this apple orchard by Penna et al. (2021). Measuring the water stable isotopic composition, these authors showed that the tree isotopic composition partially overlapped with the isotopic composition of the topsoil (0.25 m depth), which was significantly different from that of groundwater, suggesting a negligible contribution of the latter.

The results of Experiment 2 shed additional light on the low likelihood of the first possible explanation. Experiment 2 was designed to create a simplified model, under pot conditions, where the sources of tree water were only two, namely the water already present in the shoots before starting the experiment and the soil water. As the contribution of soil water uptake to total water in both the shoot axes and leaves was similar in the two experiments, we speculate that the water uptake from the deepest soil layers (<0.6 m depth) did not account for a significant fraction of shoot water that was not derived from the 0–0.6 m soil layer. We cannot, however, rule out the possibility that the capillary rise contributed to the transport of some water from the water table to the deepest part of the 0–0.6 m soil layer. To be able to quantify this process, groundwater should be labeled, which is challenging under field conditions. A major flux of water due to capillary rise, however, would have caused a decrease in the shoot isotopic composition over time, which was not observed (Figs. 3 and 5).

According to the second possible explanation, our results could be explained considering that a significant fraction of the cryogenically-extracted shoot water was not ascribable to recently root-absorbed water. This explanation is plausible if it is assumed that, to a certain extent, water is compartmentalized within tree organs (Cernusak et al., 2016; Zwieniecki et al., 2007). To support this explanation, the mechanisms of water transport and distribution within plants need to be examined. It is reasonable to assume that water moves inside the tree mainly through an apoplastic pathway, even though transcellular and symplastic movements are also plausible and the extent of each mechanism may vary according to several factors including plant species (Sack and Holbrook, 2006). In Experiment 1, the shoot axes (collected at 9 AM) contained an amount of water similar to its dry weight (56.7% FW): part of that water might have been contained in the xylem vessels, while it is reasonable to assume that another water fraction was present in the other secondary xylem tissues, namely the fibers, the fiber-tracheids, and the ray-parenchyma, as well as in the cambium, the secondary phloem and the bark (Pratt, 1990). In the leaves, the main xylem vessels split into progressively smaller veins, embedded in leaf mesophyll. Water movements along pathways outside the veins are rather complicated and still partially unknown (Barbour et al., 2017). Similarly, a precise identification of the position of evaporation sites is difficult, although most of the evaporation processes occur at the intercellular spaces, with the resulting water vapor diffusing to the atmosphere through the stomata (Cronquist, 1971). In Experiment 1, the leaf (collected at 9 AM) water content was 65% of the leaf fresh weight, and it is likely that most of the water was present in the veins, the palisade cells, and the spongy mesophyll, with the latter two tissues accounting for most of the apple leaf volume (Pratt, 1990).

If an equilibrium process existed in the soil between pre-event and recently absorbed water, considering the potential evapotranspiration during the experimental period of the field experiment in the range of ca. 7 L day^{-1} $tree^{-1}$, we would have observed a gradual increase in the isotopic composition of shoots from day 1 to day 7, with a final isotopic composition close to that of soil water at 0–0.6 m depth. Since this was not observed, we speculate that in the short period, apple trees featuring no water stress dis did not significantly exchange and mix pre-event and recently absorbed water, neither in the shoot axes nor in the leaves. In light of this explanation, the fact that the total water content of leaves was around 9% higher than that of shoot axes could explain the lower δ^2H values found in the leaves as compared to the shoot axes. To which extent water mixing processes within tree organs depends on the fact that trees did not suffer limitations in water supply and were not exposed to a high evaporative demand deserves further investigation.

This study represents a first attempt to trace irrigation water in an apple orchard and to quantify the contribution of irrigation water to tree water during the summer season. We are aware that factors such as the local soil texture, climate, as well the type of irrigation system make our results site-specific, and thus further studies in different settings are needed before our conclusions can be generalized to other apple orchards.

5. Conclusions

The two labeling experiments with ^2H-enriched water under field and pot conditions shed light on the fate of the irrigation water in the soil and the apple tree in an Alpine orchard. As expected, most of the irrigation water was present in the 0–0.2 m soil layers, but the labeled water also infiltrated until 0.6 m depth.

The uptake of irrigation water by apple trees in the field was rather rapid as indicated by the presence of labeled water in the shoots at 1.5–2.5 m height already after 2–4 h after the water supply. The presence of a superficial root system might explain the rapid uptake of labeled water. The contribution of irrigation water to shoot water increased during the first day after the irrigation, but then leveled off, reaching a maximum of 7.8% and 3.3% in shoot axes and leaves, respectively. Such low values are not surprising considering the large water pool in the soil and the fact that irrigation water mixed with pre-event soil water. Considering that the labeled water was localized in the 0–0.6 m soil layer, where also around 90% of the fine roots were present, we estimated that at the end of the experiment shoot axes and leaves contained, on average, 48 ± 3% and 26 ± 2% of labeled water taken up from such a layer, respectively. As indicated by the ancillary pot experiment a significant fraction of the cryogenically-extracted shoot water was already present before the starting of the experiment and it mixed at very low rates with the recently absorbed labeled water, probably due to the combination of low transpiration rates and the presence of highly available soil water. It is unlikely that the water fraction unaccounted by the water uptake from the 0–0.6 m soil layer largely derived from unlabeled water taken up by the roots in the deepest soil layer (> 0.6 m), although the capillary rise from the shallow water table could have contributed to the soil moisture at the bottom of the 0–0.6 m soil layer.

In light of our results, it is evident that water mixing processes at the soil and tree level are still not fully understood. This knowledge gap affects the ability to elaborate appropriate eco-hydrological models useful both for environmental studies and a sustainable irrigation management.

Funding

This work was supported by the Department of Innovation, Research

and University of the Autonomous Province of Bozen-Bolzano within the NOI Capacity Building II funding frame (Decision 864, 04.09.2018). The authors thank the Department of Innovation, Research and University of the Autonomous Province of Bozen-Bolzano for covering the Open Access publication costs.

Declaration of Competing Interest

The authors declare that they have no known competing financial interests or personal relationships that could have appeared to influence the work reported in this paper.

Acknowledgments

The authors thank Ulrich Innerhofer, the land owner, for the availability in allowing field work and Christian Ceccon at the Free University of Bozen-Bolzano for the IRMS analysis.

Appendix A. Supporting information

Supplementary data associated with this article can be found in the online version at doi:10.1016/j.agwat.2022.107572.

References

Adams, R.E., Hyodo, A., SantaMaria, T., Wright, C.L., Boutton, T.W., West, J.B., 2020. Bound and mobile soil water isotope ratios are affected by soil texture and mineralogy, whereas extraction method influences their measurement. Hydrol. Process. 34, 991–1003. https://doi.org/10.1002/hyp.13633.

Allen, R.G., Pereira, L.S., Raes, D., Smith, M., 1998. FAO Irrigation and drainage paper No. 56, Rome: Food and Agriculture Organization of the United Nations.

Allen, R.G., Pruitt, W.O., Wright, J.L., Howell, T.A., Ventura, F., Snyder, R., Itenfisu, D., Steduto, P., Berengena, J., Yrisarry, J.B., Smith, M., Pereira, L.S., Raes, D., Perrier, A., Alves, I., Walter, I., Elliott, R., 2006. A recommendation on standardized surface resistance for hourly calculation of reference ET_0 by the FAO56 Penman-Monteith method. Agric. Water Manag. 81, 1–22. https://doi.org/10.1016/j.agwat.2005.03.007.

Araguás-Araguás, L., Rozanski, K., Gonfiantini, R., Louvat, D., 1995. Isotope effects accompanying vacuum extraction of soil water for stable isotope analyses. J. Hydrol. 168, 159–171. https://doi.org/10.1016/0022-1694(94)02636-P.

Barbeta, A., Jones, S.P., Clavé, L., Wingate, L., Gimeno, T.E., Fréjaville, B., Wohl, S., Ogée, J., 2019. Unexplained hydrogen isotope offsets complicate the identification and quantification of tree water sources in a riparian forest. Hydrol. Earth Syst. Sci. 23, 2129–2146. https://doi.org/10.5194/hess-23-2129-2019.

Barbeta, A., Gimeno, T.E., Clavé, L., Fréjaville, B., Jones, S.P., Delvigne, C., Wingate, L., Ogée, J., 2020. An explanation for the isotopic offset between soil and stem water in a temperate tree species. New Phytol. 227, 766–779. https://doi.org/10.1111/nph.16564.

Barbeta, A., Burlett, R., Martín-Gómez, P., Fréjaville, B., Devert, N., Wingate, L., Domec, J., Ogée, J., 2022. Evidence for distinct isotopic compositions of sap and tissue water in tree stems: consequences for plant water source identification. New Phytol. 233, 1121–1132. https://doi.org/10.1111/nph.17857.

Barbour, M.M., Farquhar, G.D., Buckley, T.N., 2017. Leaf water stable isotopes and water transport outside the xylem. Plant. Cell Environ. 40, 914–920. https://doi.org/10.1111/pce.12845.

Becker, M.W., Coplen, T.B., 2001. Use of deuterated water as a conservative artificial groundwater tracer. Hydrogeol. J. 9, 512–516. https://doi.org/10.1007/s100400100157.

Benettin, P., Nehemy, M.F., Cernusak, L.A., Kahmen, A., McDonnell, J.J., 2021. On the use of leaf water to determine plant water source: a proof of concept. Hydrol. Process 35. https://doi.org/10.1002/hyp.14073.

Berry, Z.C., Evaristo, J., Moore, G., Poca, M., Steppe, K., Verrot, L., Asbjornsen, H., Borma, L.S., Bretfeld, M., Hervé-Fernández, P., Seyfried, M., Schwendenmann, L., Sinacore, K., De Wispelaere, L., McDonnell, J., 2018. The two water worlds hypothesis: addressing multiple working hypotheses and proposing a way forward. Ecohydrology 11, e1843. https://doi.org/10.1002/eco.1843.

Berry, Z.C., Emery, N.C., Gotsch, S.G., Goldsmith, G.R., 2019. Foliar water uptake: processes, pathways, and integration into plant water budgets. Plant. Cell Environ. 42, 410–423. https://doi.org/10.1111/pce.13439.

Beyer, M., Penna, D., 2021. On the spatio-temporal under-representation of isotopic data in ecohydrological studies. Front. Water 3, 1–9. https://doi.org/10.3389/frwa.2021.643013.

Beyer, M., Koeniger, P., Gaj, M., Hamutoko, J.T., Wanke, H., Himmelsbach, T., 2016. A deuterium-based labeling technique for the investigation of rooting depths, water uptake dynamics and unsaturated zone water transport in semiarid environments. J. Hydrol. 533, 627–643. https://doi.org/10.1016/j.jhydrol.2015.12.037.

Beyer, M., Hamutoko, J.T., Wanke, H., Gaj, M., Koeniger, P., 2018. Examination of deep root water uptake using anomalies of soil water stable isotopes, depth-controlled isotopic labeling and mixing models. J. Hydrol. 566, 122–136. https://doi.org/10.1016/j.jhydrol.2018.08.060.

Bogie, N.A., Bayala, R., Diedhiou, I., Conklin, M.H., Fogel, M.L., Dick, R.P., Ghezzehei, T. A., 2018. Hydraulic redistribution by native Sahelian shrubs: bioirrigation to resist in-season drought. Front. Environ. Sci. 6, 1–12. https://doi.org/10.3389/fenvs.2018.00098.

Cao, X., Yang, P., Engel, B.A., Li, P., 2018. The effects of rainfall and irrigation on cherry root water uptake under drip irrigation. Agric. Water Manag. 197, 9–18. https://doi.org/10.1016/j.agwat.2017.10.021.

Cernusak, L.A., Barbour, M.M., Arndt, S.K., Cheesman, A.W., English, N.B., Feild, T.S., Helliker, B.R., Holloway-Phillips, M.M., Holtum, J.A.M., Kahmen, A., Mcinerney, F. A., Munksgaard, N.C., Simonin, K.A., Song, X., Stuart-Williams, H., West, J.B., Farquhar, G.D., 2016. Stable isotopes in leaf water of terrestrial plants. Plant Cell Environ. 39, 1087–1102. https://doi.org/10.1111/pce.12703.

Chartzoulakis, K., Bertaki, M., 2015. Sustainable water management in agriculture under climate change. Agric. Agric. Sci. Procedia 4, 88–98. https://doi.org/10.1016/j.aaspro.2015.03.011.

Clothier, B.E., Green, S.R., Deurer, M., 2007. Preferential flow and transport in soil: Progress and prognosis. Eur. J. Soil Sci. 59, 2–13. https://doi.org/10.1111/j.1365-2389.2007.00991.x.

Cronquist, A., 1971. Introductory Botany, second ed. Harper and Row, New York.

Di Bonito, M., Breward, N., Crout, N., Smith, B., Young, S., 2008. Overview of selected soil pore water extraction methods for the determination of potentially toxic elements in contaminated soils: operational and technical aspects. In: De Vivo, B., Belkin, H.E., Lima, A. (Eds.), Environmental Geochemistry. Elsevier, pp. 213–249. https://doi.org/10.1016/B978-0-444-53159-9.00010-3.

Doorenbos, J., Pruitt, W.O., 1977. Crop water requirements. Irrigation and drainage paper no. 24, (rev.). Rome, Italy.

Ehleringer, J.R., Dawson, T.E., 1992. Water uptake by plants: perspectives from stable isotope composition. Plant. Cell Environ. 15, 1073–1082. https://doi.org/10.1111/j.1365-3040.1992.tb01657.x.

Ellsworth, P.Z., Williams, D.G., 2007. Hydrogen isotope fractionation during water uptake by woody xerophytes. Plant Soil 291, 93–107. https://doi.org/10.1007/s11104-006-9177-1.

Farquhar, G.D., Cernusak, L.A., Barnes, B., 2007. Heavy water fractionation during transpiration. Plant Physiol. 143, 11–18. https://doi.org/10.1104/pp.106.093278.

Gan, K.S., Wong, S.C., Yong, J.W.H., Farquhar, G.D., 2002. ^{18}O spatial patterns of vein xylem water, leaf water, and dry matter in cotton leaves. Plant Physiol. 130, 1008–1021. https://doi.org/10.1104/pp.007419.

Gazis, C., Feng, X., 2004. A stable isotope study of soil water: Evidence for mixing and preferential flow paths. Geoderma 119, 97–111. https://doi.org/10.1016/S0016-7061(03)00243-X.

Genereux, D., 1998. Quantifying uncertainty in tracer-based hydrograph separations. Water Resour. Res. 34, 915–919. https://doi.org/10.1029/98WR00010.

Grashey-Jansen, S., 2010. Pedohydrological case study of two apple-growing locations in South Tyrol (Italy). Agric. Water Manag. 98, 234–240. https://doi.org/10.1016/j.agwat.2010.08.012.

Gröning, M., 2018. Performance assessment of stable isotope ratio measurements for highly enriched and highly depleted water samples by laser spectrometry, Technical Note.

Grünberger, O., Michelot, J.L., Bouchaou, L., Macaigne, P., Hsissou, Y., Hammecker, C., 2011. Capillary rise quantifications based on in-situ artificial deuterium peak displacement and laboratory soil characterization. Hydrol. Earth Syst. Sci. 15, 1629–1639. https://doi.org/10.5194/hess-15-1629-2011.

Jackisch, C., Knoblauch, S., Blume, T., Zehe, E., Hassler, S.K., 2020. Estimates of tree root water uptake from soil moisture profile dynamics. Biogeosciences 17, 5787–5808. https://doi.org/10.5194/bg-17-5787-2020.

Koeniger, P., Leibundgut, C., Link, T., Marshall, J.D., 2010. Stable isotopes applied as water tracers in column and field studies. Org. Geochem. 41, 31–40. https://doi.org/10.1016/j.orggeochem.2009.07.006.

Koeniger, P., Marshall, J.D., Link, T., Mulch, A., 2011. An inexpensive, fast, and reliable method for vacuum extraction of soil and plant water for stable isotope analyses by mass spectrometry. Rapid Commun. Mass Spectrom. 25, 3041–3048. https://doi.org/10.1002/rcm.5198.

Li, T., Hao, X., Kang, S., 2014. Spatiotemporal variability of soil moisture as affected by soil properties during irrigation cycles. Soil Sci. Soc. Am. J. 78, 598–608. https://doi.org/10.2136/sssaj2013.07.0269.

Liu, S., Zhang, Q., Liu, J., Sun, J., Wei, Q., 2014. Effect of partial root-zone irrigating deuterium oxide on the properties of water transportation and distribution in young apple trees. J. Integr. Agric. 13, 1268–1275. https://doi.org/10.1016/S2095-3119(13)60623-1.

Liu, Z., Ma, F., Hu, T., Zhao, K., Gao, T., Zhao, H., Ning, T., 2020. Using stable isotopes to quantify water uptake from different soil layers and water use efficiency of wheat under long-term tillage and straw return practices. Agric. Water Manag. 229, 105933 https://doi.org/10.1016/j.agwat.2019.105933.

Mahindawansha, A., Orlowski, N., Kraft, P., Rothfuss, Y., Racela, H., Breuer, L., 2018. Quantification of plant water uptake by water stable isotopes in rice paddy systems. Plant Soil 429, 281–302. https://doi.org/10.1007/s11104-018-3693-7.

Mali, N., Urbanc, J., Leis, A., 2007. Tracing of water movement through the unsaturated zone of a coarse gravel aquifer by means of dye and deuterated water. Environ. Geol. 51, 1401–1412. https://doi.org/10.1007/s00254-006-0437-4.

Maruyama, S., Tada, Y., 2014. Comparison of water isotope analysis between cavity ring-down spectroscopy and isotope ratio mass spectrometry. Geochem. J. 48, 105–109. https://doi.org/10.2343/geochemj.2.0282.

Millar, C., Pratt, D., Schneider, D.J., McDonnell, J.J., 2018. A comparison of extraction systems for plant water stable isotope analysis. Rapid Commun. Mass Spectrom. 32, 1031–1044. https://doi.org/10.1002/rcm.8136.

Montagnani, L., Zanotelli, D., Tagliavini, M., Tomelleri, E., 2018. Timescale effects on the environmental control of carbon and water fluxes of an apple orchard. Ecol. Evol. 8, 416–434. https://doi.org/10.1002/ece3.3633.

Orlowski, N., Breuer, L., McDonnell, J.J., 2016a. Critical issues with cryogenic extraction of soil water for stable isotope analysis. Ecohydrology 9, 1–5. https://doi.org/10.1002/eco.1722.

Orlowski, N., Pratt, D.L., McDonnell, J.J., 2016b. Intercomparison of soil pore water extraction methods for stable isotope analysis. Hydrol. Process. 30, 3434–3449. https://doi.org/10.1002/hyp.10870.

Penna, D., Stenni, B., Šanda, M., Wrede, S., Bogaard, T.A., Michelini, M., Fischer, B.M.C., Gobbi, A., Mantese, N., Zuecco, G., Borga, M., Bonazza, M., Sobotková, M., Čejková, B., Wassenaar, L.I., 2012. Technical note: evaluation of between-sample memory effects in the analysis of δ^2H and $\delta^{18}O$ of water samples measured by laser spectroscopes. Hydrol. Earth Syst. Sci. 16, 3925–3933. https://doi.org/10.5194/hess-16-3925-2012.

Penna, D., Geris, J., Hopp, L., Scandellari, F., 2020. Water sources for root water uptake: Using stable isotopes of hydrogen and oxygen as a research tool in agricultural and agroforestry systems. Agric. Ecosyst. Environ. 291, 106790 https://doi.org/10.1016/j.agee.2019.106790.

Penna, D., Zanotelli, D., Scandellari, F., Aguzzoni, A., Engel, M., Tagliavini, M., Comiti, F., 2021. Water uptake of apple trees in the Alps: where does irrigation water go? Ecohydrology 14. https://doi.org/10.1002/eco.2306.

Poca, M., Coomans, O., Urcelay, C., Zeballos, S.R., Bodé, S., Boeckx, P., 2019. Isotope fractionation during root water uptake by Acacia caven is enhanced by arbuscular mycorrhizas. Plant Soil 441, 485–497. https://doi.org/10.1007/s11104-019-04139-1.

Pratt, C., 1990. Apple trees: morphology and anatomy. In: Janick, J. (Ed.), Horticultural Reviews. Timber Press, Portland, Oregon, pp. 265–305. https://doi.org/10.1002/9781118060858.ch6.

Rasmussen, C.R., Thorup-Kristensen, K., Dresbøll, D.B., 2020. Uptake of subsoil water below 2 m fails to alleviate drought response in deep-rooted Chicory (Cichorium intybus L.). Plant Soil 446, 275–290. https://doi.org/10.1007/s11104-019-04349-7.

Rothfuss, Y., Javaux, M., 2017. Reviews and syntheses: Isotopic approaches to quantify root water uptake: a review and comparison of methods. Biogeosciences 14, 2199–2224. https://doi.org/10.5194/bg-14-2199-2017.

Rowland, D.L., Leffler, A.J., Sorensen, R.B., Dorner, J.W., Lamb, M.C., 2008. Testing the efficacy of deuterium application for tracing water uptake in peanuts. Trans. ASABE 51, 455–461. https://doi.org/10.13031/2013.24387.

Sack, L., Holbrook, N.M., 2006. Leaf hydraulics. Annu. Rev. Plant Biol. 57, 361–381. https://doi.org/10.1146/annurev.arplant.56.032604.144141.

Schreel, J.D.M., Steppe, K., 2020. Foliar water uptake in trees: negligible or necessary? Trends Plant Sci. 25, 590–603. https://doi.org/10.1016/j.tplants.2020.01.003.

Seeger, S., Weiler, M., 2021. Temporal dynamics of tree xylem water isotopes: in situ monitoring and modeling. Biogeosciences 18, 4603–4627. https://doi.org/10.5194/bg-18-4603-2021.

Sheshshayee, M.S., Bindumadhava, H., Ramesh, R., Prasad, T.G., Lakshminarayana, M. R., Udayakumar, M., 2005. Oxygen isotope enrichment ($\Delta^{18}O$) as a measure of time-averaged transpiration rate. J. Exp. Bot. 56, 3033–3039. https://doi.org/10.1093/jxb/eri300.

Song, X., Gao, X., Dyck, M., Zhang, W., Wu, P., Yao, J., Zhao, X., 2018. Soil water and root distribution of apple tree (*Malus pumila Mill*) stands in relation to stand age and rainwater collection and infiltration system (RWCI) in a hilly region of the Loess Plateau, China. CATENA 170, 324–334. https://doi.org/10.1016/j.catena.2018.06.026.

Sprenger, M., Leistert, H., Gimbel, K., Weiler, M., 2016. Illuminating hydrological processes at the soil-vegetation-atmosphere interface with water stable isotopes. Rev. Geophys. 54, 674–704. https://doi.org/10.1002/2015RG000515.

Sprenger, M., Llorens, P., Cayuela, C., Gallart, F., Latron, J., 2019. Mechanisms of consistently disjunct soil water pools over (pore) space and time. Hydrol. Earth Syst. Sci. 23, 2751–2762. https://doi.org/10.5194/hess-23-2751-2019.

Thielemann, L., Gerjets, R., Dyckmans, J., 2019. Effects of soil-bound water exchange on the recovery of spike water by cryogenic water extraction. Rapid Commun. Mass Spectrom. 33, 405–410. https://doi.org/10.1002/rcm.8348.

Tsuruta, K., Yamamoto, H., Katsuyama, M., Kosugi, Y., Okumura, M., Matsuo, N., 2019. Effects of cryogenic vacuum distillation on the stable isotope ratios of soil water. Hydrol. Res. Lett. 13, 1–6. https://doi.org/10.3178/hrl.13.1.

Vargas, A.I., Schaffer, B., Yuhong, L., Sternberg, L. da S.L., 2017. Testing plant use of mobile vs immobile soil water sources using stable isotope experiments. New Phytol. 215, 582–594. https://doi.org/10.1111/nph.14616.

Villalobos, F.J., Fereres, E., 2016. Principles of agronomy for sustainable agriculture. Principles of Agronomy for Sustainable Agriculture. Springer International Publishing, New York, NY, USA. https://doi.org/10.1007/978-3-319-46116-8.

Wassenaar, L.I., Ahmad, M., Aggarwal, P., Duren, M., Pöltenstein, L., Araguas, L., Kurttas, T., 2012. Worldwide proficiency test for routine analysis of δ^2H and $\delta^{18}O$ in water by isotope-ratio mass spectrometry and laser absorption spectroscopy. Rapid Commun. Mass Spectrom. 26, 1641–1648. https://doi.org/10.1002/rcm.6270.

Wu, H., Li, J., Zhang, C., He, B., Zhang, H., Wu, X., Li, X.-Y., 2018. Determining root water uptake of two alpine crops in a rainfed cropland in the Qinghai Lake watershed: first assessment using stable isotopes analysis. F. Crop. Res. 215, 113–121. https://doi.org/10.1016/j.fcr.2017.10.011.

Wu, X., Zheng, X.-J., Yin, X.-W., Yue, Y.-M., Liu, R., Xu, G.-Q., Li, Y., 2019. Seasonal variation in the groundwater dependency of two dominant woody species in a desert region of Central Asia. Plant Soil 444, 39–55. https://doi.org/10.1007/s11104-019-04251-2.

Zanotelli, D., Montagnani, L., Andreotti, C., Tagliavini, M., 2019. Evapotranspiration and crop coefficient patterns of an apple orchard in a sub-humid environment. Agric. Water Manag. 226, 105756 https://doi.org/10.1016/j.agwat.2019.105756.

Zanotelli, D., Montagnani, L., Andreotti, C., Tagliavini, M., 2022. Water and carbon fluxes in an apple orchard during heat waves. Eur. J. Agron. 134, 126460 https://doi.org/10.1016/j.eja.2022.126460.

Zhang, Y., Zhang, Z., Ma, Z., Chen, J., Akbar, J., Zhang, S., Che, C., Zhang, M., Cerdà, A., 2018. A review of preferential water flow in soil science. Can. J. Soil Sci. 98, 604–618. https://doi.org/10.1139/cjss-2018-0046.

Zhao, L., Wang, L., Cernusak, L.A., Liu, X., Xiao, H., Zhou, M., Zhang, S., 2016. Significant difference in hydrogen isotope composition between xylem and tissue water in *Populus Euphratica*. Plant. Cell Environ. 39, 1848–1857. https://doi.org/10.1111/pce.12753.

Zheng, W., Wen, M., Zhao, Z., Liu, J., Wang, Z., Zhai, B., Li, Z., 2017. Black plastic mulch combined with summer cover crop increases the yield and water use efficiency of apple tree on the rainfed Loess Plateau. PLoS One 12, e0185705. https://doi.org/10.1371/journal.pone.0185705.

Zwieniecki, M.A., Brodribb, T.J., Holbrook, N.M., 2007. Hydraulic design of leaves: insights from rehydration kinetics. Plant, Cell Environ. 30, 910–921. https://doi.org/10.1111/j.1365-3040.2007.001681.x.